A relativistic continuum Hartree-Bogoliubov theory description of N=3 isotones*

HAN Rui(韩瑞) JI Juan-Xia(姬娟霞) LI Jia-Xing(李加兴)[1)]

School of Physical Science and Technology, Southwest University, Chongqing 400715, China

Abstract: The ground-state properties of N=3 isotones and mirror nuclei have been investigated in the Rrelativistic Continuum Hartree-Bogoliubov theory with the NLSH effective interaction. Pairing correlations are taken into account by a density-dependent δ-force. The calculations show that the proton density distributions of ^{8}B and ^{9}C have a long tail, the core has an increasing tendency of ^{9}C and the paired off valence protons make the halo distribution shrink. The cross sections for the ^{8}B(^{9}C)+^{12}C reaction which are consistent with the experimental data are calculated using the Glauber model. On the whole, we think that ^{8}B is a one-proton halo nucleus and ^{9}C is a two-proton halo nucleus.

Key words: relativistic continuum Hartree-Bogoliubov, proton halo, N=3 isotones, cross section

PACS: 21.10.Gv, 21.10.Dr, 25.60.Dz **DOI:** 10.1088/1674-1137/35/9/006

1 Introduction

Since the experimental progress in radioactive nuclear beam facilities many exotic nuclei have been produced [1–5]. It has enabled us to study exotic nuclei far from the β-stability line and make it possible to determine the nuclear size for unstable nuclei, mainly based on the reaction cross section. One of the most interesting findings is the observation of the neutron halo structure in some light atomic nuclei, in which the rms matter radius is much larger than that expected from the conventional mass dependence $1.2A^{1/3}$ [1]. Due to the confining effects of the Coulomb barrier, the nuclei exhibiting proton halos are not so common. Nevertheless, there is a number of candidates along the proton drip line, such as the ground-states of ^{8}B [6–11], ^{17}Ne [12–14] ^{20}Mg [15], ^{23}Al [16–18], $^{26-28}$P, ^{27,28}S [19, 20].Therefore, much more efforts are required to reveal the mechanism for the formation of proton halo structure in proton-rich nuclei.

At present, the proton-rich nucleus ^{8}B [7–9] has been taken as a good candidate of proton halo nuclei. Compared with ^{8}B, ^{9}C is one more proton-rich nucleus, so its nuclear structure has attracted more attention. Earlier experiments have been carried out by measuring the interaction cross sections of ^{8}B and ^{9}C with different targets to establish its halo nature [21, 22]. However, in these experiments, it was difficult to determine the formation mechanism of the nuclear halo.

On the theoretical side, very different models, such as the relativistic mean-field (RMF) theory [23, 24], the Skyrme Hartree-Fock theory [11, 25] and the relativistic continuum Hartree-Bogoliubov (RCHB) theory [26] in particular, have been extensively applied with great success to many nuclear phenomena of drip-line nuclei in recent years [26–28]. In this work, in order to well explain the microscopic structure of the halo and the effect of increscent core upon a halo-nucleus, we will study the properties of N=3 isotones and mirror nuclei with the RCHB theory. Particular interest will be focused on the coupling between the valance nucleon and the core and the interaction cross section. The strength V_0 of the pairing force for the protons is fixed to 325 MeV. Because of the block effect, the pairing correlations of neutrons and odd nucleus are strongly suppressed and

Received 9 December 2010

* Supported by Fundamental Research Funds for Cental Universities (XDJK2010D005, XDJK2010C049) and National Natural Science Foundation of China (11075133, 10205019)

1) E-mail: lijx@swu.edu.cn

thus neglected. The set of effective interaction NLSH is used to examine the influence of interaction on the halo structure.

2 The model

In the RCHB theory, the particle-hole (ph) and particle-particle (pp) correlations are described in an unified way on a mean-field level by using two average potentials: the self-consistent mean field that encloses all the long range ph correlations and a pairing field $\hat{\Delta}$ which sums up the pp-correlations. The ground state of a nucleus is described by a generalized Slater determinant $|\Phi\rangle$ that represents the vacuum with respect to independent quasiparticles ($\alpha_{\rm k}^{+}$), which are related to the single-nucleon creation ($c_{\rm l}^{+}$) and annihilation ($c_{\rm l}$) operators through the unitary Bogoliubov transformation,

$$\alpha_{\rm k}^{+}=\sum_{\rm l} U_{\rm lk}c_{\rm l}^{+}+V_{\rm lk}c_{\rm l}, \tag{1}$$

where U and V are the Hartree-Bogoliubov wave functions determined by the solution of the RCHB equation. In the coordinate representation:

$$\begin{pmatrix} h_{\rm D}-m-\lambda & \Delta \\ -\Delta^{*} & -h_{\rm D}^{*}+m+\lambda \end{pmatrix}\times\begin{pmatrix} U_{\rm k}(\boldsymbol{r}) \\ V_{\rm k}(\boldsymbol{r})\end{pmatrix}$$

$$= E_{\rm k}\begin{pmatrix} U_{\rm k}(\boldsymbol{r}) \\ V_{\rm k}(\boldsymbol{r})\end{pmatrix}, \tag{2}$$

where m is the nucleon mass and the chemical potential λ is determined by the particle number subsidiary condition in order that the expectation value of the particle number operator in the ground state equals the number of nucleons. The column vectors denote the quasiparticle wave functions and $E_{\rm k}$ are the quasiparticle energies. The self-consistent mean-field corresponds to the single-nucleon Dirac Hamiltonian $\hat{h}_{\rm D}$. In the usual meson-exchange representation and for the stationary case with time-reversal symmetry, i.e. for the ground-state of an even-even nucleus:

$$\hat{h}_{\rm D}=\alpha\cdot\boldsymbol{p}+\beta(m+g_{\sigma}\sigma)+g_{\omega}\omega^{0}+g_{\rho}\tau_{3}\rho^{0}+e\frac{1-\tau_{3}}{2}A^{0}. \tag{3}$$

The classical meson fields σ, ω and ρ are the solutions of the stationary Klein-Gordon equations.

The pairing correlations are taken into account by a density dependent force of zero range [29],

$$V^{\rm pp}(r_1,r_2)=V_0\delta(r_1,r_2)\frac{1}{4}(1-\sigma_1\sigma_2)\left[1-\frac{\rho(r)}{\rho_0}\right], \tag{4}$$

where ρ_0 is taken as 0.152 fm^{-3} as usual.

The pairing field Δ in Eq. (2) is given by

$$\Delta_{ab}(\boldsymbol{r},\boldsymbol{r}')=\frac{1}{2}\sum_{c,d}V_{abcd}(\boldsymbol{r},\boldsymbol{r}')\kappa_{cd}(\boldsymbol{r},\boldsymbol{r}'). \tag{5}$$

where $\kappa=U^{*}V^{\rm T}$ is the pairing tensor and $V_{abcd}(\boldsymbol{r},\boldsymbol{r}')$ are the matrix elements of the two-body pairing interaction. The indices a, b, c and d denote the quantum numbers that specify the Dirac indices of the spinor.

The RCHB equations are solved in a self-consistent way by the shooting method and the Runge-Kutta algorithm with a step size of 0.1 fm using proper boundary conditions in a spherical box of radius $R=20$ fm. The number of continuum levels is restricted by introducing a cutoff energy of 120 MeV. More details are given in Ref. [29].

3 Results and discussions

The calculated matter radius $r_{\rm m}$ and experimental data are presented in Fig. 1. The calculated results are in good agreement with the experimental data. There is an obvious increase of matter radius for ^{8}B

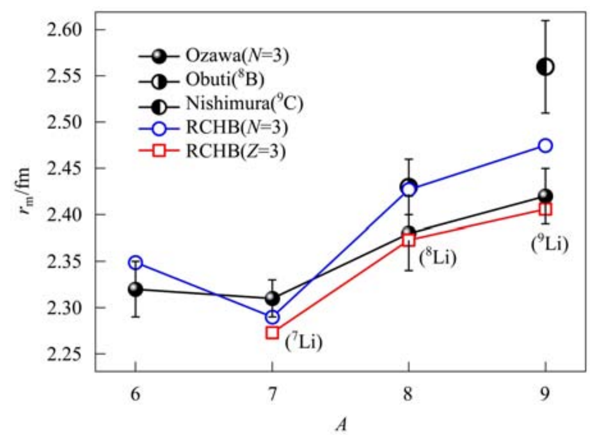

Fig. 1. (color online) Matter rms radius ($r_{\rm m}$) for N=3 isotones (blue empty circles) and mirror nuclei (red empty squares). RCHB calculations are compared with experimental data (black dots).

Table 1. The comparison of calculated binding energy, rms radius of neutron, proton and matter with the experimental data [21, 30].

	B(exp)/MeV	B(cal)/MeV	$r_{\rm n}$/fm	$r_{\rm p}$/fm	$r_{\rm m}$/fm	$r_{\rm m}$(exp)/fm
^{9}C	39.037	38.539	2.09	2.65	2.475	2.42±0.03
^{8}B	37.737	34.642	2.12	2.59	2.427	2.38±0.04
^{7}Be	37.600	36.910	2.18	2.37	2.290	2.31±0.02
^{6}Li	31.944	28.844	2.32	2.38	2.349	2.32±0.03
^{9}Li	45.341	45.649	2.55	2.08	2.406	2.32±0.02
^{8}Li	41.277	39.045	2.51	2.13	2.373	2.37±0.02
^{7}Li	39.244	38.966	2.33	2.20	2.273	2.33±0.02

and ^{9}C. In Table 1, we have presented the properties of the ground state of N=3 isotones and mirror nuclei. The calculated binding energy is consistent with the experimental value.

In Fig. 2, it is clearly seen that the proton density has a long tail in respect of the neutron density for ^{8}B and ^{9}C. Fig. 3 shows the logarithmic and nonlogarithmic coordinate density distributions of ^{9}C and ^{8}B. We can find that the proton density distribution tail of ^{8}B is more widely extended than ^{9}C (the logarithmic coordinate presenting it), while its radius is smaller. That is mainly because the core of ^{8}B is smaller than ^{9}C (the nonlogarithmic coordinate presenting it). Also, the coupling between the core and the valence nucleons probably made their core structure change correspondingly.

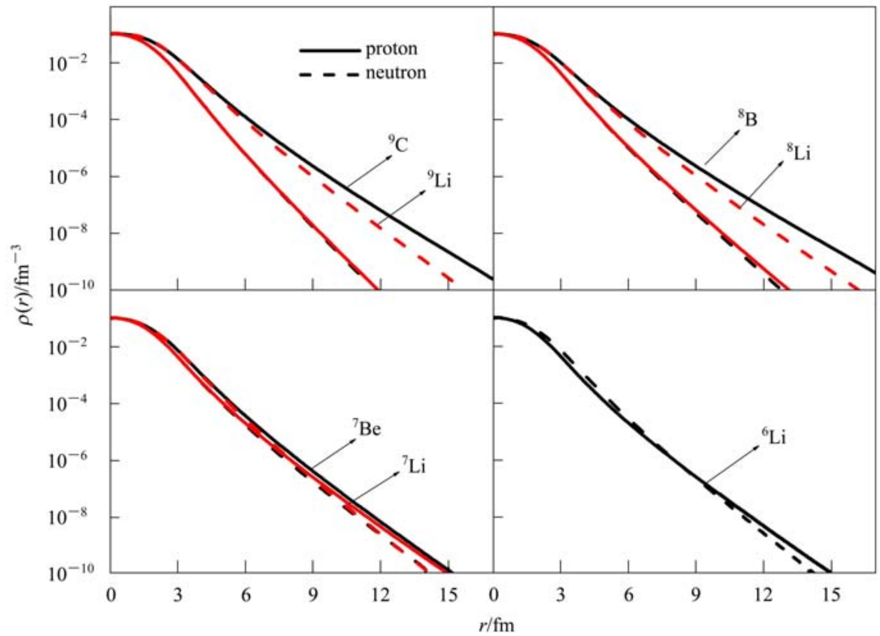

Fig. 2. (color online) The density distributions of proton (solid) and neutron (dashed) in N=3 isotones (black line) and mirror nuclei (red line).

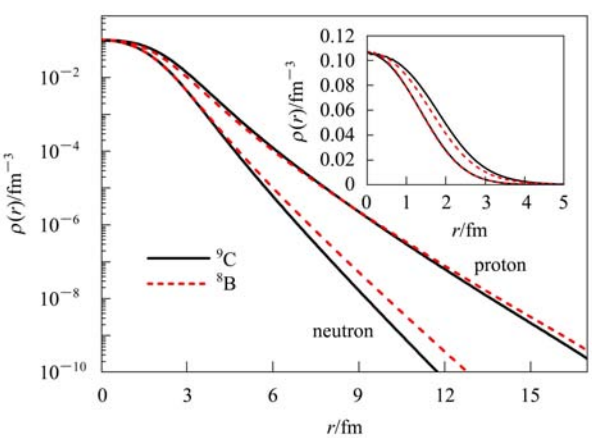

Fig. 3. (color online) The density distributions of proton and neutron in ^{9}C (black solid) are compared with ^{8}B (red dashed). The inset shows the nonlogarithmic coordinate density distributions of ^{9}C and ^{8}B.

The single particle energy levels are given in Fig. 4. The Fermi level for the protons is very close to the continuum limit and the paring correlations cause a partial occupation of the $1p_{1/2}$ level for ^{9}C. Additionally, the contributions of the $1p_{1/2}$ and $1p_{3/2}$ channel to the matter radius have an obvious increase (^{9}C: $1s_{1/2}$ 1.876, $1p_{3/2}$ 2.947, $1p_{1/2}$ 3.303; ^{8}B: $1s_{1/2}$ 1.865, $1p_{3/2}$ 2.981; unit: fm). Moreover, the two-proton separation energy

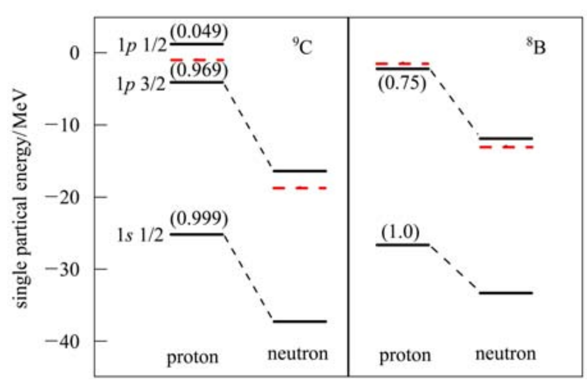

Fig. 4. The energy levels of proton (left panel) and neutron (right panel) for ^{9}C and ^{8}B. The dashed line is Fermi surface. The date in bracket shows the particle occupying weight of the corresponding level.

(S^{2p}=1.4 MeV) is greatly close to the one-proton separation energy (S^{p}=1.3 MeV) of ^{9}C. It means that the last two protons of ^{9}C are paired off [31], which influence the halo distribution and make the halo distribution shrink and the core structure different from ^{8}B's change. Combing the above discussions, we consider ^{8}B is a one-proton halo nucleus, while ^{9}C is a two-proton halo nucleus. The proton halo is formed mostly by the occupied valence proton level $p_{3/2}$ with a small orbital angular momentum, correspondingly small centrifugal barrier and weak binding.

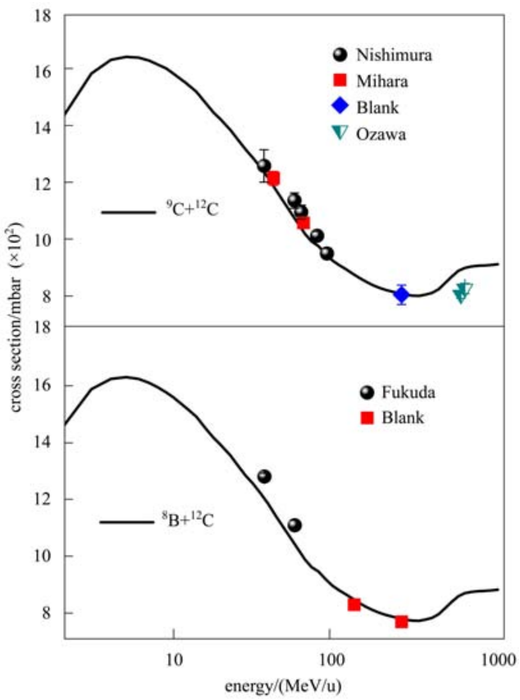

Fig. 5. The ^{8}B (^{9}C)+^{12}C excitation curves obtained by substituting the density distributions of RCHB theory calculation into the Glauber model and comparison with the experimental data.

In Fig. 5, the cross sections based on the Glauber model calculations with the density obtained from RCHB are directly compared with the experimental data. The experimental results indicate that ^{8}B and ^{9}C are proton halo nuclei. Our calculated results are in very good agreement with the experimental data. It gives a consistent description of the proton and neutron distribution and could examine the development of proton halo.

4 Summary

The ground-state properties of N=3 isotones and mirror nuclei have been investigated using the RCHB theory with the NLSH effective interaction. Pairing correlations are taken into account by a density-dependent δ-force. The calculations show that the proton density distributions of ^{8}B and ^{9}C have a long tail, the core has an increasing tendency of ^{9}C and the paired off valence protons make the halo distribution shrink. The cross sections for the ^{8}B(^{9}C)+^{12}C reaction are calculated using the Glauber model. The agreement between the Glauber model calculations and the experimental data are very fine. On the whole, we think that ^{8}B is a one-proton halo nuclei and ^{9}C is a two-proton halo nuclei. The proton halo could be examined by the Glauber model calculations. The deformation of the core is very important for these light drip-line nuclei. Future work will focus on the study of deformation effects from these exotic nuclei.

References

1 Tanihata I et al. Phys. Rev. Lett., 1985, **55**: 2676
2 Riisager K. Rev. Mod. Phys., 1994, **66**: 1105
3 Hansen P G, Jensen A S, Jonson B. Ann. Rev. Nucl. Part. Sci., 1995, **45**: 505
4 Tanihata I. Prog. Part. Nucl. Phys., 1995, **35**: 505
5 Jensen A S et al. Rev. Mod. Phys., 2004, **76**: 215
6 Negoita F et al. Phys. Rev. C, 1996, **54**: 1787
7 Smedberg M H, Baumann T, Aumann T et al. Phys. Lett. B, 1999, **452**: 1
8 Fukuda M et al. Nucl. Phys. A, 1999, **656**: 209
9 Guimaraes V et al. Phys. Rev. Lett., 2000, **84**: 1862
10 Carstoiu F et al. Phys. Rev. C, 2001, **63**: 054310
11 Chandel S S, Dhiman S K, Shyam R. Phys. Rev. C, 2003, **68**: 054320
12 Ozawa A et al. Phys. Lett. B, 1994, **334**: 18
13 Zhukov M V, Thompson I J. Phys. Rev. C, 1995, **52**: 3505
14 LU F et al. Chin. Phys. C (HEP & NP), 2009, **33**: 170
15 Suzuki T, Geissel H, Bochkarev O et al. Nucl. Phys. A, 1997, **616**: 286c
16 Ozawa A et al. Phys. Rev. C, 2006, **74**: 021301
17 CHEN J G et al. Chin. Phys. Lett., 2004, **21**: 2140
18 FANG D Q et al. Chin. Phys. Lett., 2005, **22**: 572
19 REN Z Z, CHEN B Q, MA Z Y, XU G. Phys. Rev. C, 1996, **53**: R572
20 WANG Z J et al. Science in China. G, 2003, **33**: 385
21 Ozawa A et al. Nucl. Phys. A, 1996, **608**: 63
22 Blank B et al. Nucl. Phys. A, 1997, **624**: 242
23 Lecture Notes in Physics. edited by Lalazissis G A, Ring P, Vretenar D. Springer-Verlag, Heidelberg, 2004. 641
24 Kohn W, Sham L J. Phys. Rev. A, 1965, **137**: 1697
25 BAI X H, HU J M. Phys. Rev. C, 1997, **56**: 1410
26 MENG J, Ring P. Phys. Rev. Lett., 1996, **77**: 3963
27 Poschl W et al. Phys. Rev. Lett., 1997, **79**: 20
28 MENG J. Prog. Part. Nucl. Phys., 2006, **57**: 2
29 MENG J. Nucl. Phys. A, 1998, **635**: 3
30 Audi G, Wapstra A H, Thibault C. Nucl. Phys. A, 2003, **52**: 3013
31 WANG C B et al. Comm. Theor. Phys., 2009, **51**: 895